Bulk electronic properties of $FeSi_{1-x}Ge_x$ investigated by high-resolution x-ray spectroscopies

H. Yamaoka,[1] N. Tsujii,[2] H. Oohashi,[3] D. Nomoto,[4] I. Jarrige,[5] K. Takahiro,[6] K. Ozaki,[6] K. Kawatsura,[6] and Y. Takahashi[7]

[1]*Harima Institute, The Institute of Physical and Chemical Research (RIKEN), 1-1-1 Kouto, Sayo, Hyogo 679-5148, Japan*

[2]*Quantum Beam Center, National Institute for Materials Science, 1-2-1 Sengen, Tsukuba 305-0047, Japan*

[3]*Harima Office, National Institute for Materials Science, 1-1-1 Kouto, Sayo, Hyogo 679-5148, Japan*

[4]*SPring-8 Service Co., Ltd., 2-23-1 Kouto, Sayo, Hyogo 678-1205, Japan*

[5]*Synchrotron Radiation Research Unit, Japan Atomic Energy Agency, 1-1-1 Kouto, Sayo, Hyogo 679-5148, Japan*

[6]*Kyoto Institute of Technology, Matsugasaki, Sakyo, Kyoto 606-8585, Japan*

[7]*University of Hyogo, 3-2-1 Kouto, Kamigori, Ako, Hyogo 678-1297, Japan*

(Received 27 July 2007; revised manuscript received 6 November 2007; published 5 March 2008)

We report an investigation of the bulk electronic properties of Fe in $FeSi_{1-x}Ge_x$ (x=0, 0.11, 0.19, and 0.44) measured by high-resolution x-ray absorption spectroscopy at the Fe K edge, Fe $K\beta$ x-ray emission, and $1s3p$ resonant x-ray emission spectroscopies. The emission data clearly show an increase in the magnetic moment when x increases from 0 to 0.44. This doping-induced spin transition is accompanied by the onset of the magnetic order at $x \geqslant 0.2$. The $1s3p$ resonant x-ray emission data reveal that the Fe $3d$ states exhibit a delocalized character, while no intermediate valence admixture takes place. This is at odd with the intermediate valence Kondo insulator model and rather supports the local density approximation band theory.

DOI: 10.1103/PhysRevB.77.115201 PACS number(s): 75.30.Mb, 61.05.cj, 71.20.Eh, 78.70.Ck

I. INTRODUCTION

The $B20$ cubic FeSi is a nonmagnetic p-type narrow gap semiconductor, which unconventional magnetic and transport properties have drawn considerable interest for several decades. The magnetic susceptibility was observed to increase drastically above 100 K, reaching a maximum near 540 K.[1] The magnetic behavior at high temperatures can be described by a Curie–Weiss law, indicating the presence of magnetic moment. The ~60 meV gap that opens at low temperatures was found to vanish near 250 K by means of optical conductivity measurements.[2] The gap-closure temperature being too low to result from a simple thermal activation mechanism, the Kondo insulator (KI) model was proposed to account for this behavior.[3] The formation of the ~60 meV gap at low temperatures was later confirmed by high-resolution laser photoelectron spectroscopy (PES).[4] A recent study by angle-resolved photoelectron spectroscopy on FeSi showed temperature regions of p-type semiconducting behavior at less than 100 K, intermediate and metallic states, respectively, below and above 355 K.[5]

Many models have been proposed to explain the unique properties of FeSi. These models include local density approximation (LDA),[6] extended LDA+U method,[7] two-band Hubbard model,[9,10] LDA calculations for supercells, including thermally induced lattice disorder,[11] and spin fluctuation theory.[12,13] Yamada *et al.* proposed, using band calculations, that a first-order transition occurs in the Fe $3d$ band at 170 T.[14] The band theory indicated that FeSi has a broad Fe $3d$–Si $3p$ band and both Si and Fe have neutral valences.[7,15] The band picture is, however, inconsistent with the KI model, which assumes the presence of localized $3d$ orbitals slightly hybridized with s,p levels.[7] Low temperature transport properties indicate the localization of the small amount of extrinsic carriers. The electrical resistivity, for instance, follow the variable-range-hopping form below 50 K.[8]

On the other hand, FeGe is a long-range spiral metallic ferromagnet. Thus, Ge substitution of the Si sites of FeSi offers interesting perspectives for the study of the evolution of the gap along with the semiconducting to ferromagnet metal transition.[16–23] Mani *et al.* showed pressure-induced insulator to metal transition (IMT) for x=0 and 0.05.[20] Theoretically, Anisimov *et al.* carried out LDA+U calculations on $FeSi_{1-x}Ge_x$ and predicted a first-order IMT at around x=0.4.[21] Such a transition was later observed experimentally by Yeo *et al.*[22] at x=0.25. Jarlborg performed spin-polarized band calculations for supercells of $FeSi_{1-x}Ge_x$.[23] They demonstrated an increase in the volume and disorder with x and predicted the IMT to occur at $x \geqslant 0.3$. They indicated that a small change in the volume induces a large change in the magnetic moment for large x and that a small change in the volume induces a large change in the magnetic moment for large x. The calculated density of states (DOS) and the electron phonon coupling, however, were too small for the measured specific heat, signifying the importance of the effect of spin fluctuations.[23] DiTusa *et al.* observed an IMT in Al-substituted FeSi for Al concentration $\geqslant$0.001. Though Al-substituted FeSi behavior is similar to Si:P, its quasiparticle excitations show exceptional mass enhancement around the transition reminiscent of strongly correlated systems.[24] Overall, it appears that the semiconductorlike behavior of FeSi is not well understood yet, and it is still an open question whether it can be properly described by the band theory or should be accounted for as a strongly correlated system.

Clearing up the ambiguity of the electronic states and estimating the validity of the KI model[22] call for an accurate experimental analysis of the electronic structure of this material. In this paper, we study the bulk electronic properties of Fe in $FeSi_{1-x}Ge_x$ as a function of Ge doping and temperature by means of high-resolution Fe K x-ray absorption spectroscopy, $K\beta$ x-ray emission, and $1s3p$ resonant x-ray emission spectroscopies. The x-ray emission data provide evidence for a spin crossover from low spin (LS) to high spin (HS) with increasing x. Delocalization and high degree of covalence for the Fe $3d$ states in FeSi are deduced from the $1s3p$ resonant x-ray emission spectroscopy measurements.

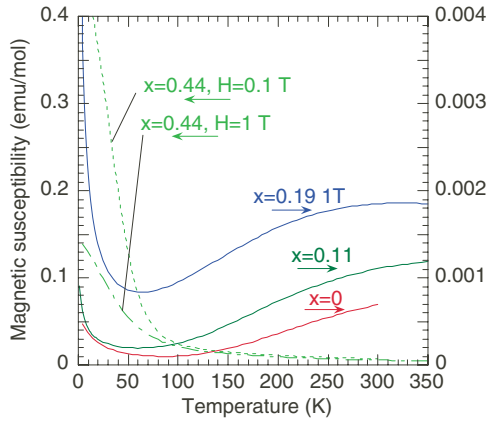

FIG. 1. (Color online) Magnetic susceptibility M/H as a function of temperature for $FeSi_{1-x}Ge_x$ (x=0, 0.11, 0.19, and 0.44).

Our results support the LDA band theory but are inconsistent with KI picture, as no intermediate valence admixture is observed.

II. EXPERIMENT

A. Samples

Polycrystalline samples of $FeSi_{1-x}Ge_x$ were prepared by argon arc melting from pure metals and annealing in evacuated silica tubes. The Si/Ge composition was determined by the energy dispersive x-ray spectroscopy. Powder x-ray diffraction confirmed that all the samples (x=0, 0.11, 0.19, and 0.44) were in single phase with the cubic $B20$ structure. The results of the magnetic susceptibility measurement as a function of temperature for x=0, 0.11, 0.19, and 0.44 are shown in Fig. 1.[25] Magnetic susceptibility of x=0, 0.11, and 0.19 show a gaplike behavior, while that of x=0.44 shows ferromagnetic transition at low temperature. This is similar to the previous results of Yeo *et al.*[22]

B. X-ray spectroscopy

X-ray absorption spectroscopy in the partial fluorescence yield mode (PFY-XAS), x-ray emission spectroscopy (XES), and resonant x-ray emission spectroscopy (RXES) measurements were performed at the BL15XU undulator beamline in SPring-8.[26] The undulator beam was monochromatized by a water-cooled double crystal monochromator, calibrated in energy between the K absorption edges of Cu, Fe, and Cr metal foils. The incident beam intensity was monitored by a thin Al foil located just before the sample. The emitted x rays were analyzed using a Ge (111) double crystal spectrometer with (+, +) geometry.[27] The lattice constant of the Ge analyzer was previously estimated[28] and the energy calibration of the spectrometer was performed with the Fe $K\alpha_1$ line of Fe metal. The resolution $E/\Delta E$ was estimated to be about 3350 at 8050 eV, where E is the emitted photon energy, and the reproducibility of the emission energy was shown to be within $\pm$0.03 eV. The emission spectra were measured with a 0.2 eV energy step but, owing to the good statistics, long-term stability of the spectrometer, and the weight of the emission profile through the curve-fitting procedure, the peak position could be determined within an accuracy of 1 order smaller than the energy step. An Iwatani CRT-M310-OP cryostat was used to cool down the samples from room temperature to about 16 K.

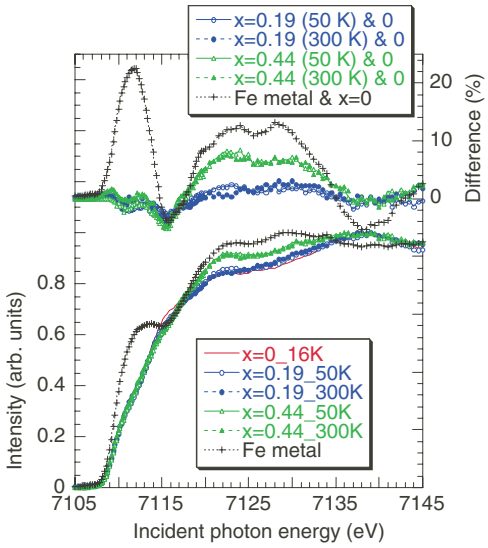

FIG. 2. (Color online) Bottom: Fe K PFY-XAS spectra for x =0 (16 K), 0.19 (50 and 300 K), and 0.44 (50 and 300 K) samples and Fe metal (300 K). The intensity is normalized to the maximum. Top: Intensity difference with the x=0 spectrum.

III. RESULTS AND DISCUSSION

A. High-resolution x-ray absorption spectroscopy

Figure 2 shows the Fe K PFY-XAS spectra for the x=0 (16 K), 0.19 (50 and 300 K), 0.44 (50 and 300 K) samples and Fe metal (300 K). They were obtained by setting the spectrometer energy to the peak of the Fe $K\alpha_1$ ($2p \rightarrow 1s$) emission line while scanning the incident energy through the Fe K edge.[29] Spectra in Fig. 2 are normalized in intensity to their maximum around 7140 eV, where we estimate the statistical error to be $\pm$0.4%. We observe no temperature dependence for the x=0.19 and 0.44 samples. The upper part of Fig. 1 shows the intensity difference between these respective spectra and the spectrum for x=0. The intensity in the 7117–7139 eV energy range gradually increases with x and tends to approach the one of Fe metal for the highest x value.

The peak at 7112 eV in the spectrum of Fe metal disappears in the spectra of $FeSi_{1-x}Ge_x$. Müller *et al.* suggested that this peak corresponds to Fe 3d density of states based on a comparison between x-ray absorption spectra obtained for 3d transition metals.[30] They pointed that the intensity of this peak decreases with increasing atomic number along the 3d transition-metal row and argued that it originates from the electronic filling of the 3d band. Based on this idea, our results suggest the filling of the 3d band for $FeSi_{1-x}Ge_x$ over Fe.

On the other hand, the preedge peak was shown to gain intensity from both the dipole-forbidden 1s-3d transition and the dipole contribution from on-site 3d-4p hybridization.[31] Furthermore, Igarashi and Hirai, through a comparison be-

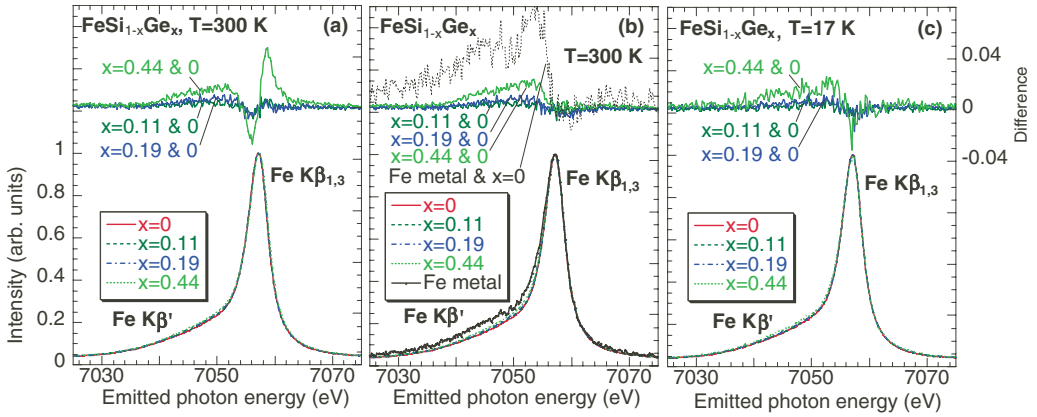

FIG. 3. (Color online) (a) Bottom: Fe $K\beta$ emission spectra as a function of x at 300 K. Top: Intensity difference with the $x=0$ spectrum. (b) Same data as (a) with the $K\beta$ peaks adjusted in energy to that of $x=0$ and with the Fe metal spectrum. (c) Fe $K\beta$ emission spectra at 17 K. The peak positions of Fe $K\beta$ are adjusted.

tween calculated and experimental magnetic circular dichroism absorption spectra on Fe metal, showed that it is the hybridization between the Fe $4p$ states of the core hole site and the Fe $3d$ states of a neighboring site which mostly contributes to the intensity of this peak.[32] The absence of a peak at 7112 eV in the $FeSi_{1-x}Ge_x$ spectra hints at a very weak p-d hybridization, which agrees well with the band calculations.[6,15]

The valence state of Fe in its intermetallic compounds is often higher than Fe metal, in which case a chemical shift is observed in the Fe K absorption edge at higher energies with respect to Fe metal.[33] In the present case, however, the maximum of the derivative of the PFY-XAS spectra for Fe metal (after subtraction of the 7112 eV preedge peak) and $FeSi_{1-x}Ge_x$ ($x=0$, 0.19, and 0.44) is nearly constant at 7109.4 ± 0.2 eV. This interestingly indicates that no change occurs in the charge state of Fe upon alloying with Si or Ge or changing temperature. We will show later that the absence of intermediate valence admixture in FeSi is confirmed by RXES. The absence of the change in the absorption edges is consistent with the band calculation for these systems, which suggested a neutral valence state (Fe^0).[6,21] As seen in Fig. 2, the PFY-XAS spectra of the $x=0.44$ sample approaches the one of Fe metal in the $E\geqslant7118$ eV region, which corresponds to the $1s\rightarrow4p$ dipolar transitions.[34]

Urasaki and Saso showed with a two-band Hubbard model that the gap of FeSi increases and the DOS near the Fermi level changes as the temperature is decreased.[10] Angle-resolved PES also showed a temperature dependence for the valence band spectra of FeSi.[5] Our PFY-XAS spectra, however, are not sensitive to temperature change, as well as the x-ray emission spectra, as will be shown later. LDA band calculations indicated that the DOS of FeSi near the Fermi level mainly results from Fe $3d$ states, slightly hybridized with the surrounding Si $3p$ orbitals.[15] Using PFY-XAS at the Fe K preedge, one does not probe the Fe $3d$ states directly but through $3d$-$4p$ hybridization.

B. X-ray emission spectroscopy

$K\beta$ emission corresponds to a $3p\rightarrow1s$ recombination after the creation of a $1s$ core hole. The exchange interaction between the $3p$ core hole and the $3d$ open shell in the final state splits the spectrum between the main line and a satellite peak, called $K\beta'$.[35] $K\beta_{1,3}$ and $K\beta'$ are usually considered to correspond to down-spin and up-spin transitions of $3p$ states, respectively. We, however, noted that up- and down-spin states are actually mixed in the spectra of $3d$ metal compounds and thus only relative changes in the spin state could be observed.[33,36] It is also noted that we always observe $K\beta'$ when the $3p$ core hole exists due to the above interaction. Thus, we can only compare the relative change in the spin states as low-spin state or high-spin state.

Figure 3(a) shows the Fe $K\beta$ spectra obtained for $x=0$, 0.1, 0.19, and 0.44 at 300 K with an incident photon energy of 7140 eV (bottom), together with the intensity difference from the $x=0$ spectrum (top). The intensities are normalized to the $K\beta_{1,3}$ peak values. Statistical error is $\pm0.7\%$ at the emitted photon energy of 7040 eV. A little shift of the order of 0.1 eV toward low photon energies is observed in the maximum of the $K\beta_{1,3}$ emissions in Fig. 3(a). Here, we define the center of mass of $K\beta$ emission as c.m. $=\int i(E)EdE/\int i(E)dE$, where $i(E)$ and E are, respectively, intensity normalized by the area $[\int i(E)dE=1]$ and the incident photon energy in eV. The change in the c.m. is only within 0.1 eV upon changes in the Ge concentration or the temperature [as will be shown later in Fig. 5(a)]. In order to focus on the intensity changes in the $K\beta'$ region, the energy of the $K\beta_{1,3}$ peaks is adjusted in energy to the $x=0$ spectrum. The corresponding spectra are displayed in Fig. 3(b) together with the Fe metal spectrum. We observe that $K\beta'$ intensity increases and gets closer to that of Fe metal with increasing Ge concentration. Figure 3(c) shows the same spectra measured at 17 K adjusted in energy. There seems to be no temperature dependence. This is confirmed in Fig. 4, where the spectra measured for the $x=0.19$ and 0.44 samples show no change throughout the 17–300 K temperature range.

We measured the $K\alpha$ ($2p$-$1s$ transition) spectra for an incident photon energy of 7140 eV.[25] The peak energy position and width of the $K\alpha$ emission were insensitive to the change in temperature or composition. We observed a narrowing of the Fe $K\alpha$ spectral width for $FeSi_{1-x}Ge_x$ compared with Fe metal, while the widths are almost the same between $x=0.19$ and 0.44.

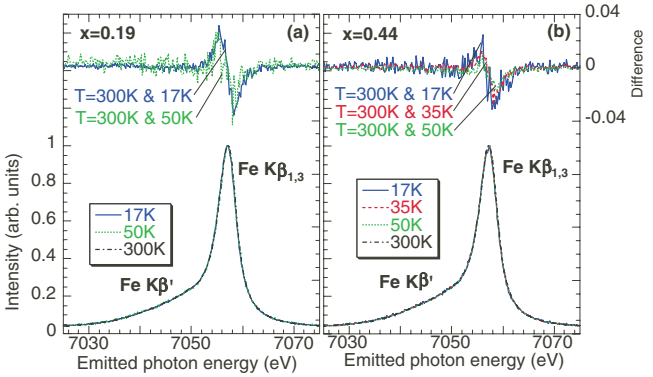

FIG. 4. (Color online) Bottom: Fe $K\beta$ emission spectra obtained at several temperatures between 17 and 300 K for (a) $x=0.19$ and (b) $x=0.44$. The peak positions are not adjusted. Top: Intensity difference between the low temperature spectra and the 300 K spectrum.

Figure 5(a) shows the c.m. at 17 and 300 K and the integrals of the absolute values of the difference (IAD)[37,38] between a given (at $x \geqslant 0$) and a reference spectrum (at $x=0$) at 300 K as a function of x. We note that, at variance with studies using external pressure,[40] the position of the c.m. shows a slight monotonous variation upon doping. The position of the c.m. in our case shows a much slighter monotonous variation upon doping. The x dependence of the IAD is linear. So far, a few methods have been proposed in order to discuss the change in the spin state based on the $K\beta$ spectra.[37–41] Among them, Vankó *et al.* recently showed that the IAD aligning on the c.m. gives satisfying results.[38] In our case though, the change in the c.m. is so small (cf. Fig. 5) that the aligning procedure does not affect the IAD significantly. Figure 5(b) summarizes the results of Figs. 3(b) and 3(c), the relative intensity change in $K\beta'$, and the peak energy shift of $K\beta_{1,3}$ with respect to $x=0$ at 17 and 300 K. In order to estimate the relative intensity changes in the $K\beta'$, we take the integral of the intensity difference with the $x=0$ spectrum in the 7030–7056 eV energy range. The $K\beta'$ intensity increases monotonously as a function of the Ge concentration. This is consistent with the result of the IAD. The $K\beta_{1,3}$ peak energy shift occurs between $x=0.19$ and $x=0.44$. No temperature dependence for the data in Fig. 5 is observed.

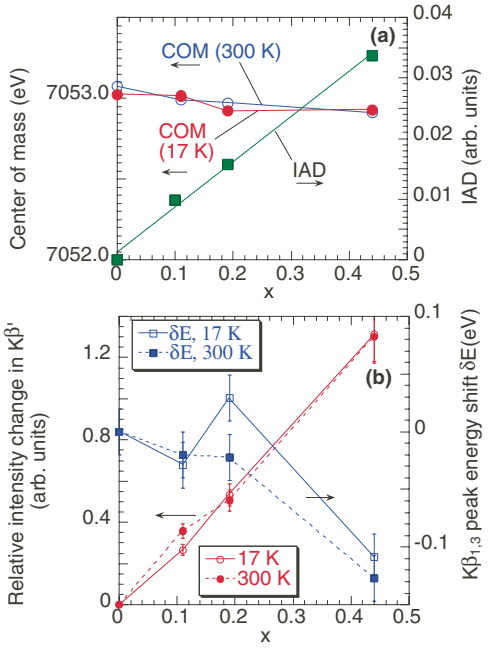

FIG. 5. (Color online) (a) Center of mass (c.m.) and integrals of the absolute values of the difference (IAD) as a function of x. (b) Intensity ratio of $K\beta'$ to $K\beta_{1,3}$ and $K\beta_{1,3}$ peak energy shift as a function of x relative to $x=0$ at 17 and 300 K.

Let us recall the general relation between the DOS and ferromagnetism according to the band picture by taking into account the electron spin states. When we increase the number of up-spin electrons by increasing the band splitting, the band energy increases by $\Delta E_0=(N_\uparrow-N_\downarrow)^2/2N(\epsilon_F)$, where $N_\uparrow$ and $N_\downarrow$ and $N(\epsilon_F)$ are- up and down-spin electron numbers and the DOS at the Fermi energy, respectively. On the other hand, the repulsive Coulomb interaction energy is lowered by $\Delta E_I=-I(N_\uparrow-N_\downarrow)^2/2$, where I is the on-site Coulomb interaction divided by the number of atoms in the crystal. When the Stoner condition of the ferromagnetic instability, $IN(\epsilon_F) \geqslant 1$, is satisfied, the sum of ΔE_0 and ΔE_I becomes negative and the ferromagnetic state with different up- and down-spin electron numbers ($N_\uparrow \neq N_\downarrow$) is stabilized. This indicates that the ferromagnetism is favored for higher intensity of DOS at the Fermi energy, i.e., for systems with narrower bandwidths. According to Yamada *et al.*, FeSi shows the first-order metamagnetic transition under around the magnetic field of 170 T.[14] This means that the ferromagnetic state of FeSi is only slightly higher in energy than the paramagnetic ground state. For supercell alloys, $FeSi_{1-x}Ge_x$, Jarlborg also showed that Ge doping causes the narrowing of the unoccupied conduction band above the gap.[23] The ferromagnetic instability around $x=0.3$ is therefore realized in terms of a discontinuous transition from the insulating regime with localized spins to the itinerant ferromagnetic state stabilized by the band narrowing. This picture is consistent with our experimental results, which show that the up-spin component increases with the Ge doping level.

A decrease in the intensity of the $K\beta'$ component has been observed in a number of transition-metal compounds subjected to external pressure.[40,42,43] This spectral change was interpreted based on the increase of the crystal field splitting $10Dq$ between the two d subbands t_{2g} and e_g under pressure, a magnetic collapse occurring as soon as $10Dq$ becomes stronger than the magnetic exchange splitting.

The lattice constant of $FeSi_{1-x}Ge_x$ was previously shown by x-ray diffraction to exhibit a monotonous increase with x up to 0.25 without structural phase transition.[17] Hence, Ge substitution of Si sites in FeSi produces a negative local chemical pressure, i.e., a local lattice expansion around Ge ions. The induced enhancement of the local density of states on the nearest neighbor Fe sites favors the appearance of magnetic moments. The increase in the $K\beta'$ intensity with Ge concentration therefore signifies the appearance of the character of local magnetic moments on Fe sites. We note that, although the spectroscopic data suggest a prolonged transition of the spin state, XES yields information about the

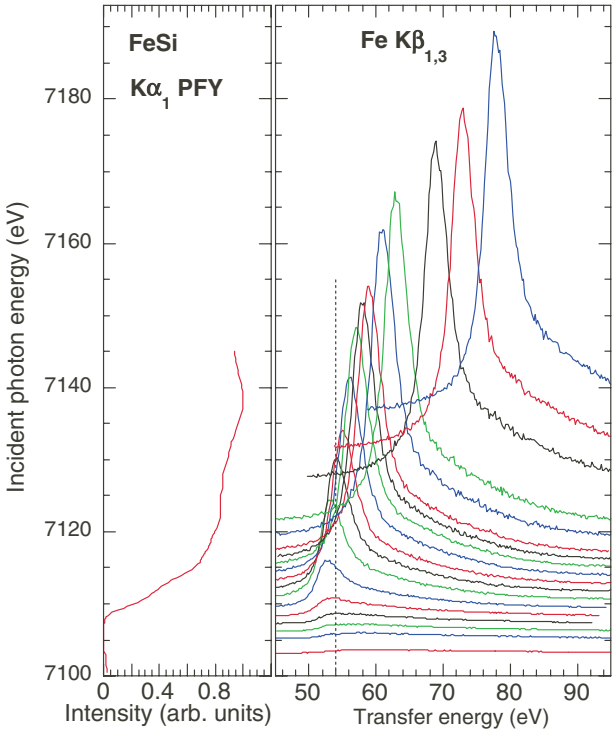

FIG. 6. (Color online) Resonant inelastic x-ray scattering of FeSi ($x=0$) for $K\beta$ at Fe K absorption edge with the PFY spectrum at 16 K.

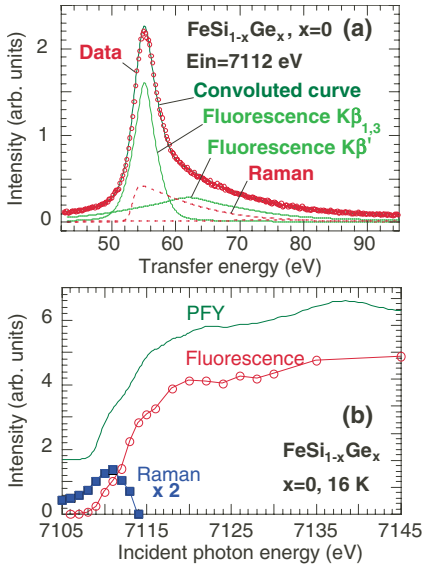

FIG. 7. (Color online) (a) Example of the curve fit for $K\beta$ emission of FeSi ($x=0$) at the incident photon energy of 7112 eV. (b) The intensities of fluorescence and Raman parts as a function of the incident photon energies at 16 K for the data in Fig. 6.

averaged local on-site magnetic moments. Thus, while apparently progressive at a macroscopic scale, this transition possibly corresponds to a superposition of nonmagnetic and magnetic Fe states, the ratio of the latter increasing with Ge doping. This view is somewhat consistent with the fact that doping causes local lattice expansions, contrasting with external pressure which induces homogeneous volume changes. $FeSi_{1-x}Ge_x$ was reported to enter a ferromagnetic phase $x=0.25$.[22] Although the present study does not include spectra in the corresponding doping range, one may anticipate the magnetic moment to increase discontinuously when entering the ferromagnetic phase at $x=0.25$.

Recently, we performed resonant photoelectron spectroscopy in the soft x-ray region for $FeSi_{1-x}Ge_x$. We will show in a separate publication[44] that the peak energy shift of the $K\beta$ emission can be related to observed changes in the valence photoelectron spectra.

C. Resonant x-ray emission spectroscopy

Figure 6 shows the $1s3p$-RXES spectra collected on FeSi at 16 K for several values of the incident energy across the Fe K absorption edge. The spectra are plotted as a function of transfer energy, which is defined as the difference between the incident and emitted photon energies. One can observe the Raman component at constant transfer energy below the edge and the growing fluorescence signal shifting toward high transfer energies as the incident energy is increased above the edge. Through a curve-fitting procedure,[28,45,46] we separate the Raman and the fluorescence components. An example of the curve fit is shown in Fig. 7(a) for an incident photon energy of 7112 eV. Here, it is noted that the $K\beta$ spectrum consists of many unresolved lines and the Raman spectrum below the absorption edge shows strong asymmetry. Therefore, for convenience, in the fitting, we assume an asymmetric profile for the Raman part and symmetric profiles for the fluorescence parts of $K\beta_{1,3}$ and $K\beta'$. The detail of the structure in the spectrum should be confirmed in the theoretical model in the future. Figure 7(b) shows the respective intensities of the Raman and fluorescence signals derived from the fit, together with the PFY-XAS spectrum. It is observed that the weak Raman component is limited to below the absorption edge, as it quickly vanishes around 7114 eV. This suggests delocalization of the Fe $3d$ band.[48]

The temperature variation of the magnetic and electronic properties of FeSi has been described until now based on the KI picture, owing to similarities between the Fe $3d$ states in FeSi and rare-earth f bands.[3] However, in most $4f$ electron systems explained by the KI picture, valence mixing is observed.[47,49,50] Yeo *et al.* compared the Hubbard-Anderson U with the hybridization between the localized and the conduction state V for FeSi.[22] They obtained a ratio U/V of 1.54, suggesting a strong valence admixture. However, as seen in Fig. 7, our fitting procedure can account for only one Raman component, suggesting that FeSi is not in an intermediate valence state. Furthermore, as mentioned in Sec. III A. A, no chemical shift is observed in the absorption edge of the PFY-XAS spectra upon Si or Ge alloying, showing that no change occurs in the charge state with respect to Fe metal. The absence of intermediate valence admixture allows us to invalidate the idea that the KI model may be suitable to explain the FeSi physical properties.

IV. CONCLUSION

We measured the bulk electronic properties of $FeSi_{1-x}Ge_x$ as a function of x and the temperature. No temperature de-

pendence is found in the electronic structure based on the Fe $K\beta_{1,3}$ XES and K PFY-XAS spectra. The $K\beta_{1,3}$ emission spectra give evidence for a doping-induced LS to HS transition between $x=0$ and 0.44. One may interpret this transition as a superposition of LS and HS states, with the former component increasing upon the doping-induced local lattice expansions. The RXES spectra suggest delocalization of the Fe $3d$ states and no intermediate valence in FeSi. The valence state is shown to remain constant upon Ge doping from the PFY-XAS measurements of the absorption edge. Our results support the LDA band theory instead of the intermediate valence state KI picture.

ACKNOWLEDGMENTS

The experiments were performed at BL15XU (Proposal No. 2006B4700) of SPring-8 in the Japan Synchrotron Radiation Research Institute. We thank H. Yoshikawa and Y. Katsuya in BL15XU for the help in the experiments and Y. Ito in Kyoto University for providing the opportunity to use the spectrometer. We also deeply appreciate T. Iwazumi in KEK and J.-P. Rueff in SOLEIL for the fruitful discussion.

[1] V. Jaccarono, G. K. Wertheim, J. H. Wernick, L. R. Walker, and S. Arajs, Phys. Rev. **160**, 476 (1967).
[2] Z. Schlesinger, Z. Fisk, H. T. Zhang, M. B. Maple, J. F. DiTusa, and G. Aeppli, Phys. Rev. Lett. **71**, 1748 (1993).
[3] G. Aeppli and Z. Fisk, Comments Condens. Matter Phys. **16**, 155 (1992).
[4] K. Ishizaka, T. Kiss, T. Shimojima, T. Yokoya, T. Togashi, S. Watanabe, C. Q. Zhang, C. T. Chen, Y. Onose, Y. Tokura, and S. Shin, Phys. Rev. B **72**, 233202 (2005).
[5] M. Arita, K. Shimada, Y. Takeda, M. Nakatake, H. Namatame, M. Taniguchi, T. Saitoh, A. Fujimori, and T. Kanomata (unpublished).
[6] L. F. Mattheiss and D. R. Hamann, Phys. Rev. B **47**, 13114 (1993).
[7] V. I. Anisimov, S. Y. Ezhov, I. S. Elfimov, I. V. Solovyev, and T. M. Rice, Phys. Rev. Lett. **76**, 1735 (1996).
[8] J. F. DiTusa, K. Friemelt, E. Bucher, G. Aeppli, and A. P. Ramirez, Phys. Rev. B **58**, 10288 (1998).
[9] C. Fu and S. Doniach, Phys. Rev. B **51**, 17439 (1995).
[10] K. Urasaki and T. Saso, J. Phys. Soc. Jpn. **68**, 3477 (1999).
[11] T. Jarlborg, Physica B **293**, 224 (2001).
[12] Y. Takahashi and T. Moriya, J. Phys. Soc. Jpn. **46**, 1451 (1979).
[13] Y. Takahashi, J. Phys.: Condens. Matter **9**, 2593 (1997); **10**, L671 (1998).; Y. Takahashi, T. Kanomata, R. Note, and T. Nakagawa, J. Phys. Soc. Jpn. **69**, 4018 (2000).
[14] H. Yamada, K. Terao, H. Ohta, T. Arioka, and E. Kulatov, J. Phys.: Condens. Matter **11**, L309 (1999).
[15] T. Jarlborg, Phys. Rev. B **51**, 11106 (1995).
[16] P. Nordblad, L. Lundgren, and O. Beckman, Phys. Scr. **28**, 246 (1983).
[17] A. Baharathi, Awadhesh Mani, G. V. Narasimha Rao, C. S. Sundar, and Y. Hariharan, Physica B **240**, 1 (1997).
[18] E. Bauer, A. Galatanu, R. Hauser, Ch. Reichl, G. Wiesinger, G. Zaussinger, M. Galli, and F. Marabelli, J. Magn. Magn. Mater. **177-181**, 1401 (1998).
[19] Ch. Reichl, G. Wiesinger, G. Zaussinger, E. Bauer, M. Galli, and F. Marabelli, Physica B **259-261**, 866 (1999).
[20] A. Mani, A. Bharathi, and Y. Hariharan, Phys. Rev. B **63**, 115103 (2001); A. Mani, Solid State Commun. **132**, 551 (2004).
[21] V. I. Anisimov, R. Hlubina, M. A. Korotin, V. V. Mazurenko, T. M. Rice, A. O. Shorikov, and M. Sigrist, Phys. Rev. Lett. **89**, 257203 (2002).
[22] S. Yeo, S. Nakatsuji, A. D. Bianchi, P. Schlottmann, Z. Fisk, L. Balicas, P. A. Stampe, and R. J. Kennedy, Phys. Rev. Lett. **91**, 046401 (2003).
[23] T. Jarlborg, J. Magn. Magn. Mater. **283**, 238 (2004).
[24] J. F. DiTusa, K. Friemelt, E. Bucher, G. Aeppli, and A. P. Ramirez, Phys. Rev. Lett. **78**, 2831 (1997).
[25] N. Tsujii, H. Yamaoka, H. Oohashi, I. Jarrige, D. Nomoto, K. Takahiro, K. Ozaki, and K. Kawatsura, Physica B (to be published).
[26] A. Nisawa, M. Okui, N. Yagi, T. Mizutani, H. Yoshikawa, and S. Fukushima, Nucl. Instrum. Methods Phys. Res. A **497**, 563 (2003).
[27] D. Horiguchi, K. Yokoi, H. Mizota, S. Sakakura, H. Oohashi, Y. Ito, T. Tochio, A. M. Vlaicu, H. Yoshikawa, S. Fukushima, H. Yamaoka, and T. Shoji, Radiat. Phys. Chem. **75**, 1830 (2006).
[28] H. Yamaoka, M. Taguchi, A. M. Vlaicu, H. Oohashi, Y. Yokoi, D. Horiguchi, T. Tochio, Y. Ito, K. Kawatsura, K. Yamamoto, A. Chainani, S. Shin, M. Shiga, and H. Wada, J. Phys. Soc. Jpn. **75**, 034702 (2006).
[29] K. Hämäläinen, D. P. Siddons, J. B. Hastings, and L. E. Berman, Phys. Rev. Lett. **67**, 2850 (1991).
[30] J. E. Müller, O. Jepsen, and J. W. Wilkins, Solid State Commun. **42**, 365 (1982).
[31] F. de Groot, Chem. Rev. (Washington, D.C.) **101**, 1779 (2001).
[32] J. I. Igarashi and K. Hirai, Phys. Rev. B **50**, 17820 (1994).
[33] H. Yamaoka, M. Oura, M. Taguchi, T. Morikawa, K. Takahiro, A. Terai, K. Kawatsura, A. M. Vlaicu, Y. Ito, and T. Mukoyama, J. Phys. Soc. Jpn. **73**, 3182 (2004).
[34] L. A. Grunes, Phys. Rev. B **27**, 2111 (1983).
[35] K. Tsutsumi, J. Phys. Soc. Jpn. **14**, 1696 (1959).
[36] X. Wang, F. M. F. de Groot, and S. P. Cramer, Phys. Rev. B **56**, 4553 (1997).
[37] G. Vankó, J.-P. Rueff, A. Mattila, Z. Németh, and A. Shukla, Phys. Rev. B **73**, 024424 (2006).
[38] G. Vankó, T. Neisius, G. Molnár, F. Renz, S. Kárpáti, A. Shukla, and F. M. de Groot, J. Phys. Chem. B **110**, 11647 (2006).
[39] J. P. Rueff, A. Shukla, A. Kaprolat, M. Krisch, M. Lorenzen, F. Sette, and R. Verbeni, Phys. Rev. B **63**, 132409 (2001).
[40] J. Badro, J.-P. Rueff, G. Vanko, G. Monaco, G. Fiquet, and F. Guyot, Science **305**, 383 (2004).
[41] P. Glatzel, U. Bergmann, F. M. F. de Groot, and S. P. Cramer, Phys. Rev. B **64**, 045109 (2001).
[42] J.-F. Lin, V. V. Struzhkin, H.-K. Mao, R. J. Hemley, P. Chow, M. Y. Hu, and J. Li, Phys. Rev. B **70**, 212405 (2004).

[43] A. Mattila, J.-P. Rueff, J. Badro, G. Vanko, and A. Shukla, Phys. Rev. Lett. **98**, 196404 (2007).
[44] H. Yamaoka, M. Matsunami, R. Eguchi, Y. Ishida, N. Tsujii, Y. Takahashi, Y. Senba, H. Ohashi, and S. Shin (unpublished).
[45] I. Jarrige, H. Ishii, Y. Q. Cai, J. P. Rueff, C. Bonnelle, T. Matsumura, and S. R. Shieh, Phys. Rev. B **72**, 075122 (2005).
[46] T. Åberg and B. Crasemann, in *Resonant Anomalous X-ray Scattering Theory and Application*, edited by G. Materlik, C. J. Sparks, and K. Fischer (Elsevier, Amsterdam, 1994), p. 431.
[47] G. H. Kwei, J. M. Lawrence, and P. C. Canfield, Phys. Rev. B **49**, 14708 (1994).
[48] J.-P. Rueff, L. Journel, P.-E. Petit, and F. Farges, Phys. Rev. B **69**, 235107 (2004).
[49] K. Shimada, Nucl. Instrum. Methods Phys. Res. A **547**, 169 (2005).
[50] M. Matsunami, T. Kiss, A. Chainani, M. Taguchi, K. Horiba, R. Eguchi, K. Yamamoto, T. Togashi, Y. Takata, K. Ishizaka, S. Watanabe, Y. Senba, H. Ohashi, S. Kunii, and S. Shin (unpublished).